Role of Multi-Electron and Multi-Orbital Effects in High-Order Harmonic Generation of Benzonitrile Molecules

Man Xing(幸满)[1,2], Jun Wang(王俊)[1,2*], Xi Zhao(赵曦)[3*], and Shushan Zhou(周书山)[4*]

[1]*Institute of Atomic and Molecular Physics, Jilin University, Changchun 130012, China*
[2]*Jilin Provincial Key Laboratory of Applied Atomic and Molecular Spectroscopy (Jilin University), Changchun 130012, China*
[3]*School of Physics and Information Technology, Shaanxi Normal University, Xi'an 710062, China*
[4]*School of Physics and Electronic Technology, Liaoning Normal University, Dalian 116029, China*

(Received 9 December 2024; accepted manuscript online 20 March 2025)

Multi-electron and multi-orbital effects play a crucial role in the interaction of strong laser fields with complex molecules. Here, multi-electron effects encompass not only electron-electron Coulomb interactions and exchange-correlation effects but also the interference between the dynamics of different electron wave packets. In this study, we employ time-dependent density functional theory to investigate high-harmonic generation in benzonitrile (C_7H_5N) subjected to intense infrared laser fields. We find that when the laser polarization direction forms a 45-degree angle with the N–C–C–C axis, the HHG signal perpendicular to this axis exhibits a significant enhancement in the 23rd–31st harmonic orders. Our analysis shows that this enhancement does not align with the classical three-step model but instead arises purely from quantum interference between different orbital channels. Our study reveals that multiple inner-shell orbitals and multi-electron effects play a crucial role in shaping this harmonic spectrum. These findings provide deeper insights into HHG mechanisms and contribute to advancements in strong-field physics and attosecond science.

DOI: 10.1088/0256-307X/42/4/043201 CSTR: 32039.14.0256-307X.42.4.043201

High-order harmonic generation (HHG) is a nonlinear optical phenomenon in which intense laser-matter interactions produce high-energy photons at integer multiples of the laser frequency.[1–6] HHG plays a crucial role in atomic and molecular physics as well as ultrafast spectroscopy,[7–9] enabling the generation of attosecond-scale ultrashort pulses and providing a powerful tool for probing the internal electronic structures of matter.[10–14]

Traditionally, HHG and molecular orbital imaging rely on the single-active-electron (SAE) approximation, which neglects essential quantum mechanical properties such as electron indistinguishability, the Pauli exclusion principle, and wave function antisymmetry.[15,16] While SAE provides useful insights in certain cases,[17,18] its limitations have become increasingly evident. For example, it fails to explain why heavier rare gases generate stronger HHG radiation than lighter ones in experiments.[19–21] By ignoring orbital coupling and electron correlation, the SAE approximation can introduce significant errors in modeling electron dynamics in complex systems.[22,23] The HHG spectrum of argon atoms, analyzed using the time-dependent configuration interaction singlet method, demonstrates that neglecting multi-orbital contributions in the 30–50 eV range can lead to a severe underestimation of the HHG yield—by up to two orders of magnitude.[24,25] In xenon atoms, collective multi-electron effects involving inner-shell electrons introduce distinct spectral features, including the giant resonance. This phenomenon arises from many-body interactions between recolliding electrons and both the outer and inner orbitals of xenon, resulting in a significant enhancement of the HHG yield.[26,27]

It is now widely recognized that molecular HHG involves multi-electron effects and multi-orbital contributions, although their full impact on HHG remains largely unexplored.[28–33] Understanding these complex dynamics is crucial for molecular orbital imaging, especially for deep orbital imaging.[34–36] Multi-electron effects and multi-orbital contributions are essential for accurately predicting and controlling spectral phenomena in HHG.[37–39] Advances in theoretical models and computational capabilities are expected to enhance our understanding of multi-electron system dynamics, further driving applications in materials science, quantum computing, and ultrafast chemistry.

In this study, we used time-dependent density functional theory to investigate high-harmonic generation in benzonitrile molecules under a linearly polarized laser field. Near the harmonic cutoff, we observed a significant enhancement in the total harmonic intensity. As the laser intensity increases, the harmonic intensity perpendicular to the N–C–C–C direction becomes dominant, resulting in a notable enhancement at specific orders. Our findings show that stronger laser fields cause ionized electrons to return more frequently to the N atomic nucleus, which is

*Corresponding author. Email: wangjun86@jlu.edu.cn; zhaoxi719@snnu.edu.cn; zhoushushan@lnnu.edu.cn
© 2025 Chinese Physical Society and IOP Publishing Ltd. All rights, including for text and data mining, AI training, and similar technologies, are reserved.

the primary contributor to this spectral feature. Analysis of high harmonics from individual orbitals revealed that this characteristic arises from the combined effects of multiple inner-shell orbitals. Our results highlight the critical role of multi-electron effects and multi-orbital contributions in the HHG of complex molecules. Studying these effects not only enhances our understanding of HHG mechanisms, strong-field physics, and quantum mechanics but also aids in predicting molecular structures and properties. This research is significant for advancing materials science, attosecond science, and ultrafast imaging.

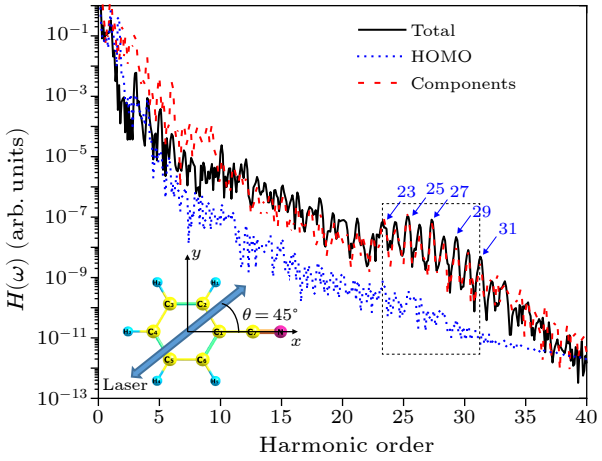

Fig. 1. The HHG spectrum of a benzonitrile molecule is shown, where the black line represents the total harmonic spectrum, and the blue line indicates the HOMO orbital spectrum. The red dashed line represents the coherent superposition of harmonics from the HOMO-2, HOMO-3, HOMO-4, HOMO-5, HOMO-11, and HOMO-12 orbitals. The inset illustrates the laser-molecule interaction, with a linearly polarized laser ($I = 1.12 \times 10^{14}\,\mathrm{W/cm^2}$, $\lambda = 800\,\mathrm{nm}$) in the x–y plane at a 45° angle to the x-axis.

We studied the HHG of benzonitrile molecules using time-dependent density functional theory. The calculations were performed in a parallelepiped box with dimensions of $60 \times 60 \times 30$, a spatial step of 0.4 a.u., and a time step of 0.04 a.u. Figure 1 shows the calculated harmonic spectrum (black curve) along with a schematic of the interaction between the benzonitrile molecules and the laser (inset). The laser field is linearly polarized with a trapezoidal envelope, featuring a rise and fall within one optical cycle (o.c.) and a 4 o.c. plateau. The laser operates at a wavelength of 800 nm and an intensity of $I = 1.12 \times 10^{14}\,\mathrm{W/cm^2}$, with the polarization direction forming a 45-degree angle with the x-axis. The total harmonic spectrum reveals an anomaly in the 23rd to 31st order harmonics (dashed box), where their intensity is significantly higher than that of adjacent harmonics. To understand the cause of this phenomenon, we calculated the harmonics of the HOMO orbital (blue dotted line in Fig. 1). The results show a mismatch with the total harmonic spectrum, as the HOMO orbital's intensity is approximately two orders of magnitude lower overall. This suggests that the HOMO orbital alone cannot account for the total harmonic spectrum, pointing to the influence of multi-orbital effects. We then included contributions from six inner orbitals (HOMO-2, HOMO-3, HOMO-4, HOMO-5, HOMO-11, and HOMO-12). Only with the combined contributions of these orbitals did the calculated spectrum align with the total harmonic spectrum. As shown by the red dashed line in Fig. 1, the harmonics of these six orbitals closely match the total spectrum within the 23rd to 31st orders. This range includes both odd- and even-order harmonics, with the latter likely arising from complex multi-orbital interactions. A detailed analysis of these interactions is beyond the scope of this study and requires further investigation.

To investigate the HHG enhancement between the 23rd and 31st harmonic orders, we calculated the intensity and phase of HHG for all orbital channels (Figs. 2 and 3). Panels (a)–(c) show odd-order harmonics, while panels (d)–(f) depict even-order harmonics. For clarity, we focus on the 23rd to 28th orders as a representative example. The peak orders in the dashed box of Fig. 1 are blue-shifted by 0.3 harmonic orders, deviating from integer values. We found that the orbitals HOMO-2, HOMO-3, HOMO-4, HOMO-5, HOMO-11, and HOMO-12 significantly contribute to this photon energy range, and the HHG interference dynamics for different orbitals vary with each harmonic order. For the 23.3rd to 28.3rd harmonics, the total harmonic intensity exceeds that of any single orbital. Figure 2 highlights the six orbitals that play a dominant role in harmonic emission, with the enhancement of harmonic intensity likely resulting from interference effects between these orbitals. Analysis of Fig. 3 shows that the enhancement of these six harmonic orders is primarily driven by the interference effects among HOMO-2, HOMO-3, HOMO-4, HOMO-5, HOMO-11, and HOMO-12. The detailed analysis is as follows: For the 23.3rd, 25.3rd, and 27.3rd harmonic orders, Figs. 2(a)–2(c) show the harmonic intensities at these three orders. The intensities of these six orbitals are comparable, indicating the need to consider interference effects. As shown in Figs. 3(a)–3(c), the phase differences among these six orbitals are nearly zero, except for HOMO-3, which exhibits a phase difference of approximately 0.3π at the 23.3rd harmonic order, but this can be neglected. Therefore, the intensity enhancement for these three harmonic orders is primarily attributed to interference effects among the six orbitals.

For the 24.3rd, 26.3rd, and 28.3rd harmonic orders, an analysis of the total harmonic intensity and the harmonic intensities of each orbital [Figs. 2(d)–2(f)] also suggests the importance of orbital interference effects. Figures 3(d)–3(f) reveal that the phase differences among the six dominant orbitals remain nearly zero. Specifically, for the 24.3rd harmonic order, HOMO-3 and HOMO-4 have phase differences of approximately 0.7π from the other orbitals, making their contributions negligible. At the 26.3rd harmonic order, HOMO-3 has a phase difference of only 0.3π from the other orbitals, and the harmonic intensity of HOMO-4 is weak, so their influence is also minimal. For the 28.3rd harmonic order, only HOMO-4 exhibits a phase difference of approximately π from the other orbitals, but its weak intensity means its influence can be disregarded.

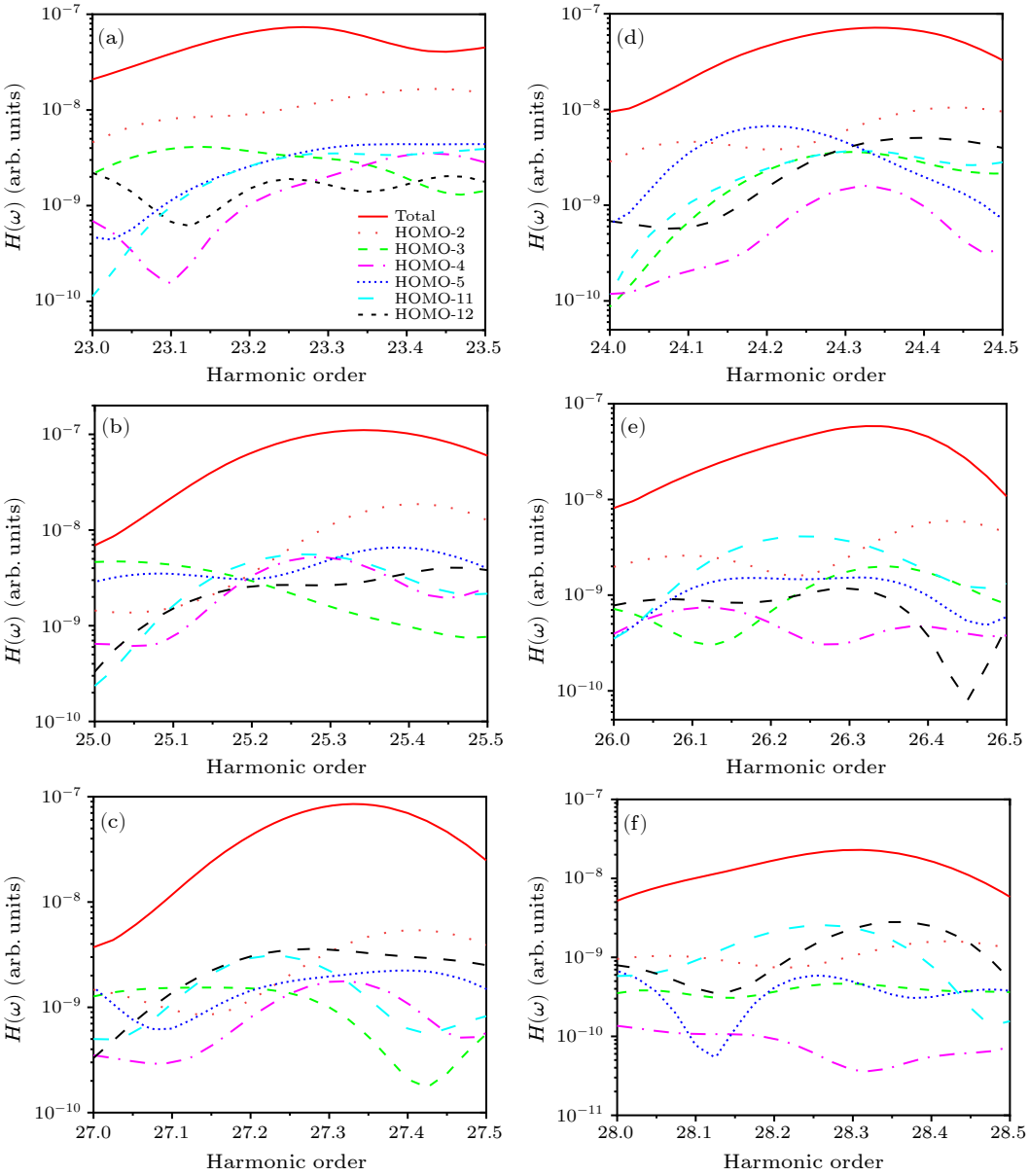

Fig. 2. Harmonic intensities of the HOMO-2, HOMO-3, HOMO-4, HOMO-5, HOMO-11, and HOMO-12 orbitals for the 23rd to 28th harmonic orders.

For comparison, we also calculated the harmonic intensity and phase of individual molecular orbitals for harmonic orders outside the dashed box in Fig. 1. The black solid lines in the figure indicate the positions of the 18th and 19th harmonics. We found that these harmonics do not exhibit the interference among the six orbitals discussed earlier. As an example, we present the intensity and phase of the 18th and 19th harmonics in Fig. 4. From Figs. 4(a) and 4(b), it can be observed that the intensity of these harmonics may be related to orbital interference. However, by analyzing the harmonic phases of different molecular orbitals [Figs. 4(c) and 4(d)], we found that their phase distribution is disordered, and the phase differences do not satisfy the conditions for constructive interference. Therefore, the generation of these harmonics is not attributed to the interference among these six molecular orbitals.

To investigate this phenomenon, we analyzed the total harmonic spectrum as well as the spectra along the x, y, and z axes [Fig. 5(a)]. The green dotted line (y direction) closely matches the total spectrum across the entire range, effectively representing it. In contrast, the red dash-dot line (x direction) shows a significant mismatch in the dashed box area, with intensities differing by up to two orders of magnitude. The cyan dashed line (z direction) is negligible, with intensities 4–8 orders of magnitude lower than the total. The harmonic enhancement from the 23rd to 31st orders primarily originates from contributions along the y direction. Time-frequency analysis [Fig. 5(b)] reveals significantly higher harmonic generation intensities at $t = 240$ a.u., $t = 350$ a.u., and $t = 460$ a.u., as indicated by the dashed lines. These three time points warrant focused analysis to better understand the system's electronic dynamics.

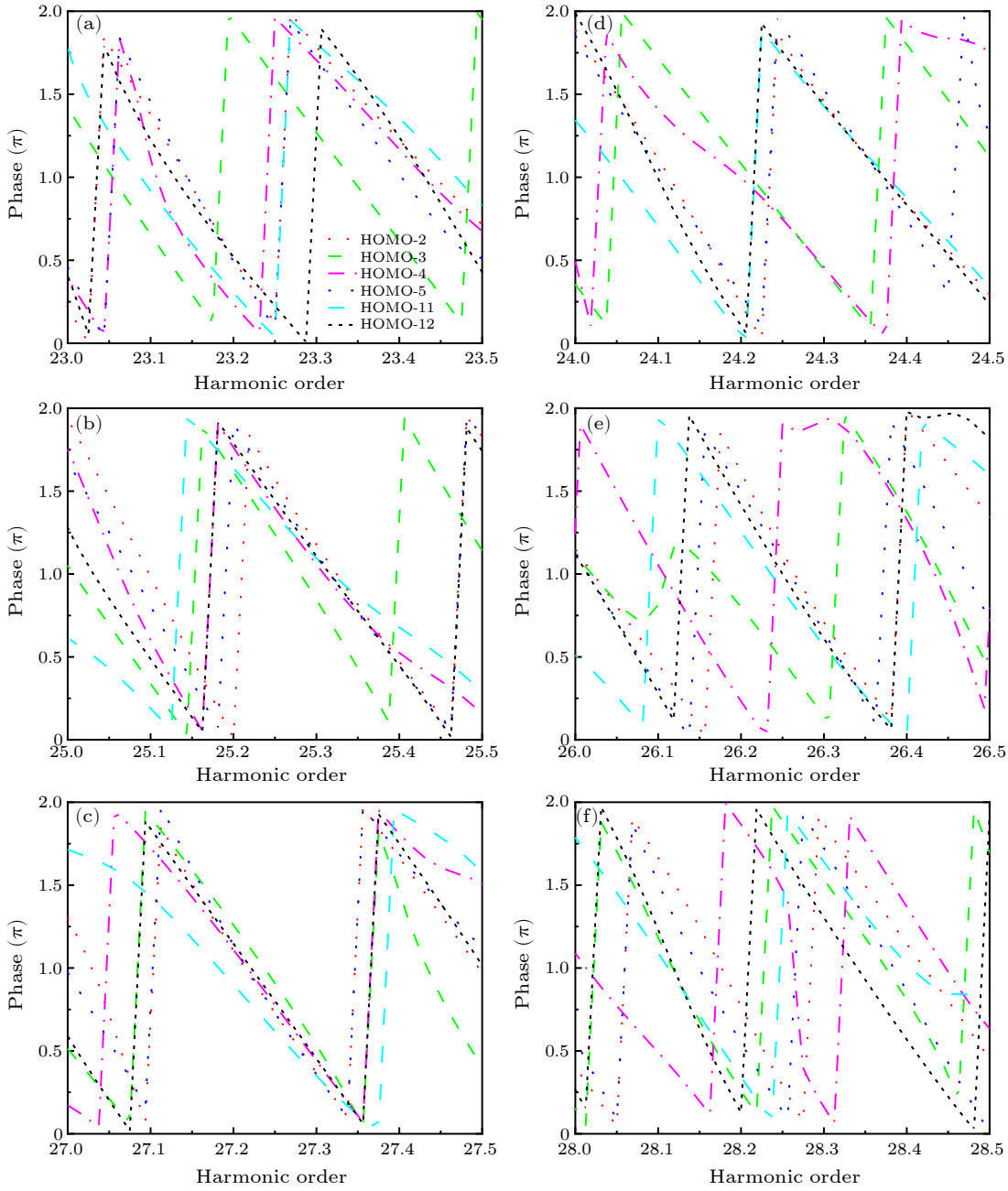

Fig. 3. Harmonic phases of the HOMO-2, HOMO-3, HOMO-4, HOMO-5, HOMO-11, and HOMO-12 orbitals for the 23rd to 28th harmonic orders.

To investigate electron dynamics, we calculated the rate of charge change around each nucleus over time. For clarity, Fig. 6(a) presents the results for N and H nuclei, while Fig. 6(b) focuses on C nuclei. The black dashed lines [from Fig. 5(b)] correspond to harmonic generation at $t = 240$ a.u., $t = 350$ a.u., and $t = 460$ a.u.. A positive charge rate indicates electron return to the region, with higher rates signifying more electron recombination, which contributes to high-order harmonic emission. Figure 6 shows that during harmonic generation, the charge rate around the N nucleus is positive and more than twice that of other nuclei, indicating a higher probability of electron return to the N nucleus. This suggests that harmonics from the 23rd to 31st orders primarily originate from electron recombination at the N atom. In strong laser fields, molecules with triple bonds (such as alkynes or certain nitrides) typically exhibit higher electron density, with electrons in π bonds being more delocalized. Compared to single and double bonds, triple bonds are more responsive to external fields. Consequently, in some cases, triple bonds may capture free electrons more easily, making the N atom more likely to attract electrons for recombination.

To further investigate the harmonic spectrum of benzonitrile, we systematically simulated the spectra at different laser intensities [Figs. 7(a)–7(c)]. As the laser intensity increases, the harmonics in the y direction pro-

gressively exceed those in the x direction and approach the total harmonic intensity. At a laser intensity of $1.12 \times 10^{14}\,\mathrm{W/cm^2}$, the y-direction harmonics dominate, suggesting that higher laser intensities enhance y-direction harmonics, driving the total intensity closer to the cutoff. Figure 7(d) shows the ionization ratios of the six molecular orbitals most significant for harmonic emission at the three laser intensities corresponding to Figs. 7(a)–7(c). As seen in Fig. 7(d), with increasing laser intensity, only HOMO-3 and HOMO-4 exhibit a reduced ionization proportion at $1.12 \times 10^{14}\,\mathrm{W/cm^2}$. This indicates that the ionization ratios of HOMO-2, HOMO-5, HOMO-6, HOMO-11, and HOMO-12 increase at this intensity, resulting in an enhanced harmonic intensity.

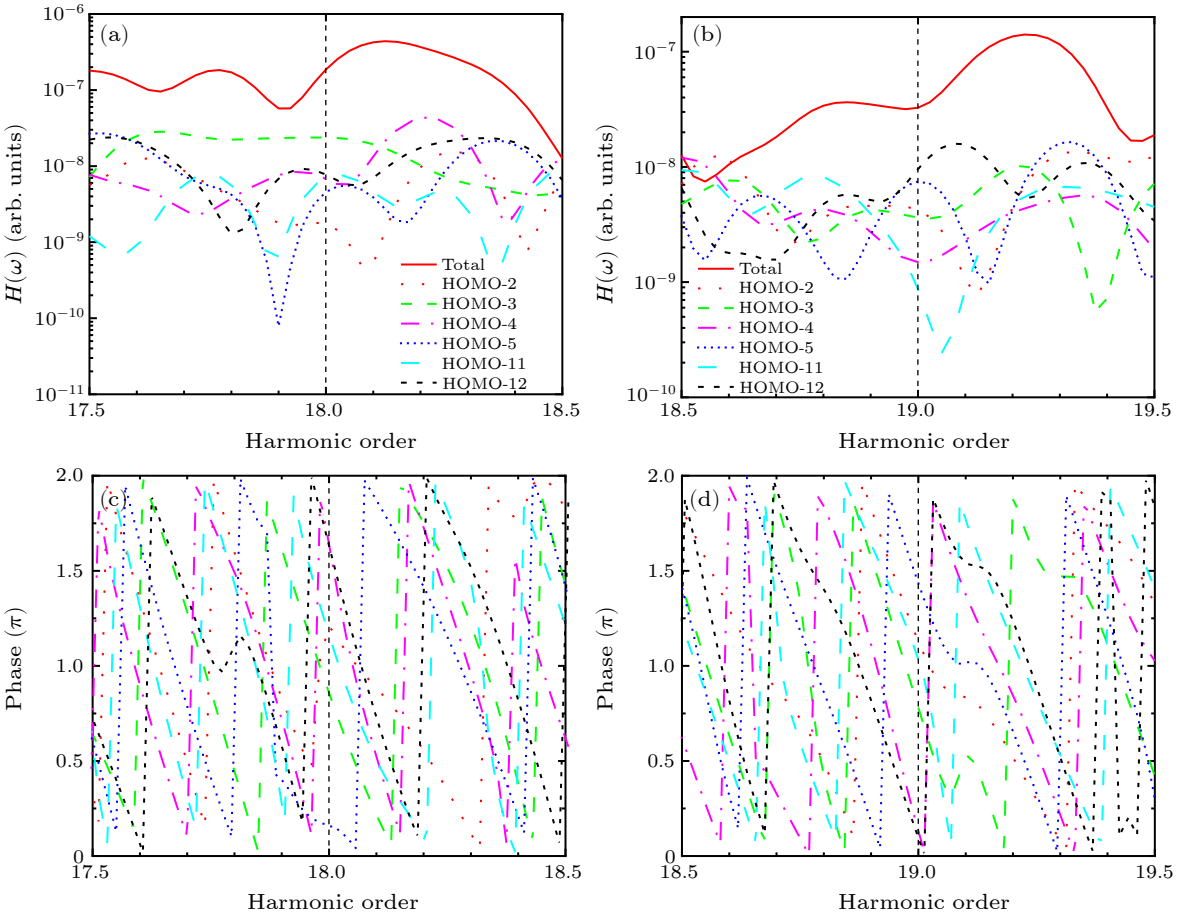

Fig. 4. Harmonic intensities and phases of the HOMO-2, HOMO-3, HOMO-4, HOMO-5, HOMO-11, and HOMO-12 orbitals near the 18th and 19th orders.

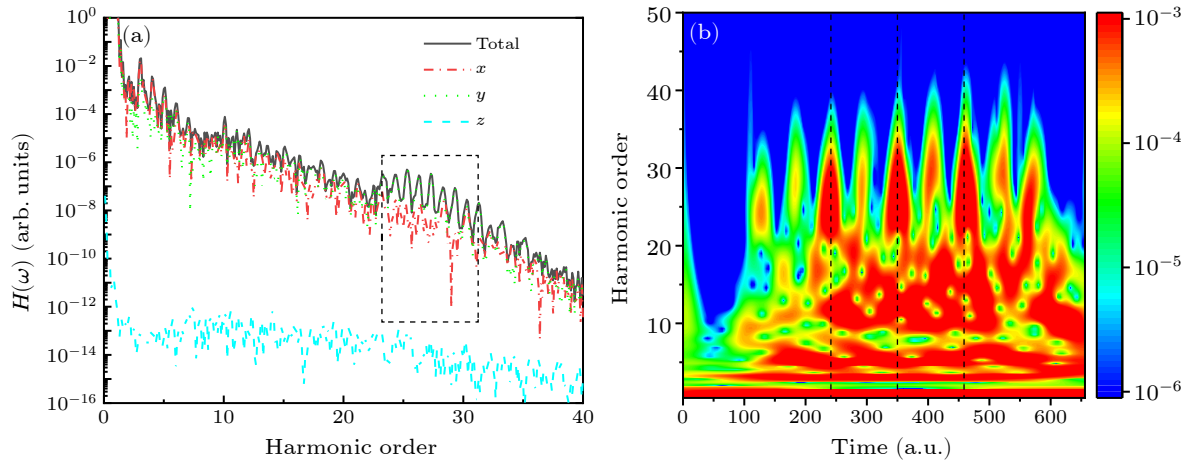

Fig. 5. (a) Total harmonic spectrum and harmonic spectra along the x, y, and z axes. (b) Time–frequency analysis of harmonic generation in the y-direction.

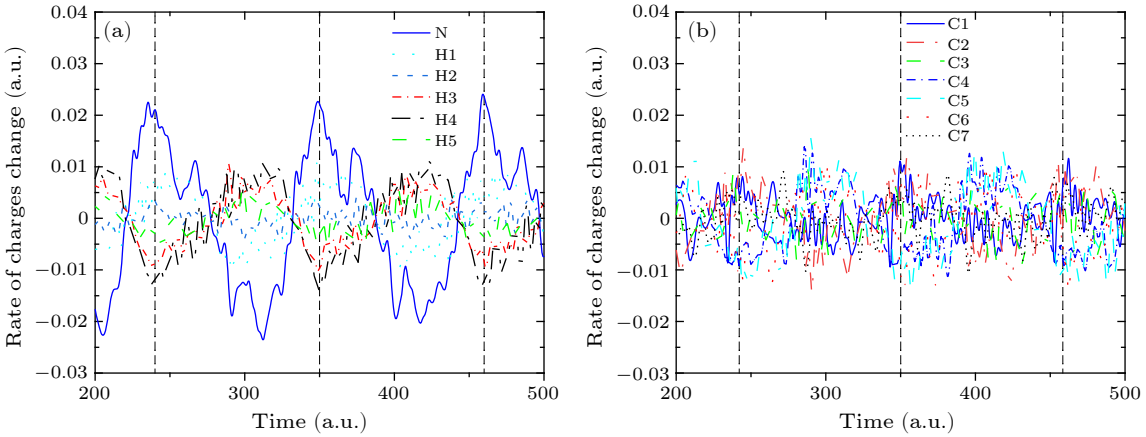

Fig. 6. Rate of charge variation around atomic nuclei: (a) N and H nuclei; (b) C nuclei.

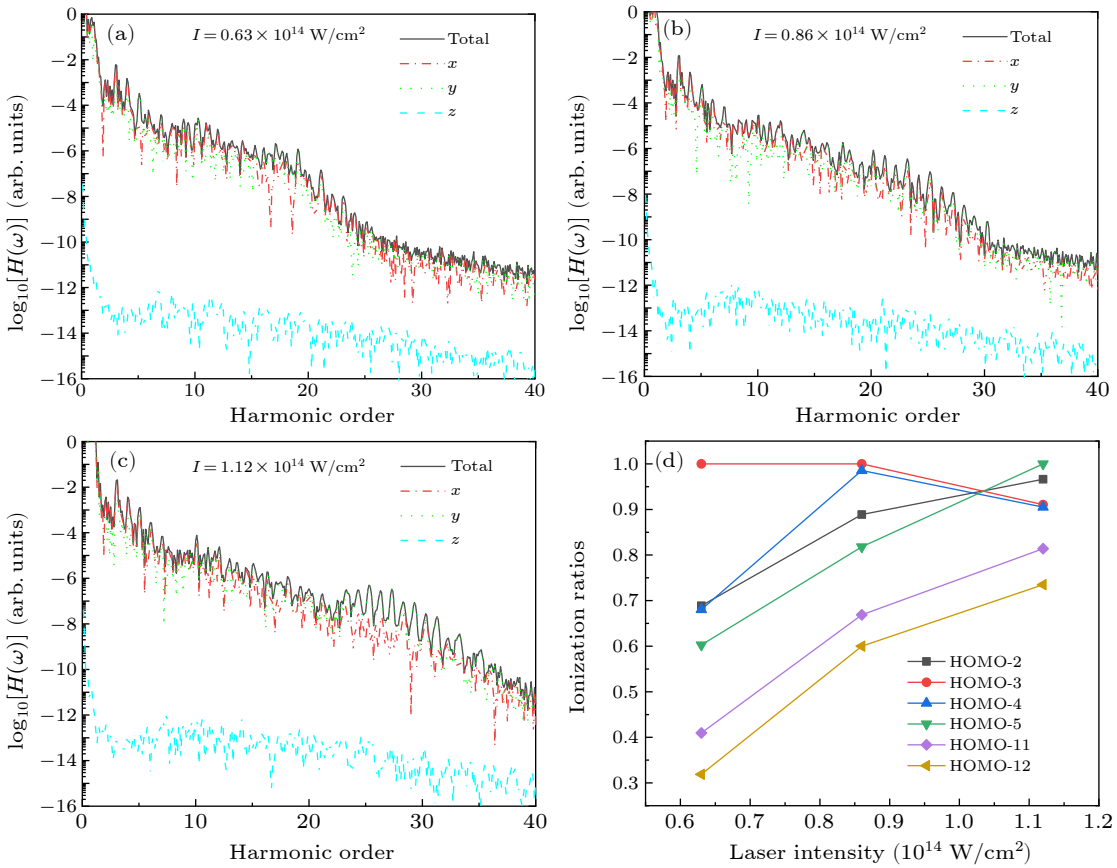

Fig. 7. Harmonic spectra along the x-, y-, and z-directions at laser intensities: (a) 0.63×10^{14} W/cm^2, (b) 0.86×10^{14} W/cm^2, and (c) 1.12×10^{14} W/cm^2. (d) Ionization ratios of various orbitals as a function of laser intensity.

In summary, we investigated the high-harmonic generation (HHG) of benzonitrile molecules under a linearly polarized laser field. Near the harmonic cutoff, we observed a significant increase in harmonic intensity. Our study identified the mechanism behind this enhancement. The total harmonics primarily originate from the y direction, driven by interference among inner orbitals (HOMO-2, HOMO-3, HOMO-4, HOMO-5, HOMO-11, and HOMO-12). These harmonics result from ionized electrons returning to and recombining with the N nucleus. This work emphasizes the critical role of multi-electron effects and multi-orbital contributions in complex molecular systems. The harmonic characteristics arise from interactions between inner orbitals, which are influenced by the return trajectories and spatial distributions of the electrons. Therefore, incorporating inner orbital contributions and multi-electron effects is crucial for studying high-order harmonic generation. We anticipate that research in this area will continue to grow, enhancing our understanding of material electronic structures and advancing quantum electronics. Additionally,

these studies will help establish accurate quantum chemical models and provide a theoretical foundation for the development of materials science and electronic technologies.

Acknowledgements. This work was supported by the National Key Research and Development Program of China (Grant No. 2022YFE0134200), the National Natural Science Foundation of China (Grant No. 12204214), the Fundamental Research Funds for the Central Universities (Grant No. GK202207012), and QCYRCXM-2022-241.

References

[1] Itatani J, Levesque J, Zeidler D, Niikura H, Pépin H, Kieffer J C, Corkum P B, and Villeneuve D M 2004 *Nature* **432** 867
[2] Krausz F, and Ivanov M 2009 *Rev. Mod. Phys.* **81** 163
[3] Henkel J, Witting T, Fabris D, Lein M, Knight P L, Tisch J W G, and Marangos J P 2013 *Phys. Rev. A* **87** 043818
[4] Vozzi C, Negro M, Calegari F, Sansone G, Nisoli M, De Silvestri S, and Stagira S 2011 *Nat. Phys.* **7** 822
[5] Qiao Y, Chen J Q, Zhou S S, Chen J G, Jiang S C, and Yang Y J 2024 *Chin. Phys. Lett.* **41** 014205
[6] Zhang C P and Miao X Y 2023 *Chin. Phys. Lett.* **40** 124201
[7] Nie Z, Guery L, Molinero E B, Juergens P, van den Hooven T J, Wang Y, Jimenez Galan A, Planken P C M, Silva R E F, and Kraus P M 2023 *Phys. Rev. Lett.* **131** 243201
[8] Yang Z, Ko C, and Ramanathan S 2011 *Annu. Rev. Mater. Res.* **41** 337
[9] Wegkamp D and Stähler J 2015 *Prog. Surf. Sci.* **90** 464
[10] Kanai T, Minemoto S, and Sakai H 2005 *Nature* **435** 470
[11] Baker S, Robinson J S, Haworth C A, Teng H, Smith R A, Chirilă C C, Lein M, Tisch J W G, and Marangos J P 2006 *Science* **312** 424
[12] Smirnova O, Mairesse Y, Patchkovskii S, Dudovich N, Villeneuve D, Corkum P, and Ivanov M Y 2009 *Nature* **460** 972
[13] Wang J, Gao S N, Liu A H, He L H, and Zhao X 2025 *Sci. Rep.* **15** 117
[14] Chen J Q, Jiang W L, Qiao Y, Yang Y J, and Chen J G 2025 *Chin. Phys. Lett.* **42** 013201
[15] Patchkovskii S, Zhao Z, Brabec T, and Villeneuve D M 2006 *Phys. Rev. Lett.* **97** 123003
[16] Schwarz W H E 2006 *Angew. Chem. Int. Ed.* **45** 1508
[17] Gordon A, Kärtner F X, Rohringer N, and Santra R 2006 *Phys. Rev. Lett.* **96** 223902
[18] Tong X M, and Chu S I 2001 *Phys. Rev. A* **64** 013417
[19] Pabst S, Greenman L, Mazziotti D A, and Santra R 2012 *Phys. Rev. A* **85** 023411
[20] Shiner A D, Schmidt B E, Trallero-Herrero C, Wörner H J, Patchkovskii S, Corkum P B, Kieffer J C, Légaré F, and Villeneuve D M 2011 *Nat. Phys.* **7** 464
[21] Santra R and Gordon A 2006 *Phys. Rev. Lett.* **96** 073906
[22] Shu Z, Liang H J, Wang Y C, Hu S L, Chen S, Xu H F, Ma R, Ding D J, and Chen J 2022 *Phys. Rev. Lett.* **128** 183202
[23] Sukiasyan S, McDonald C, Destefani C, Ivanov M Y, and Brabec T 2009 *Phys. Rev. Lett.* **102** 223002
[24] Ferré A, Boguslavskiy A E, Dagan M, Blanchet V, Bruner B D, Burgy F, Camper A, Descamps D, Fabre B, Fedorov N *et al.* 2015 *Nat. Commun.* **6** 5952
[25] Doumy G and DiMauro L F 2008 *Science* **322** 1194
[26] Boguslavskiy A E, Mikosch J, Gijsbertsen A, Spanner M, Patchkovskii S, Gador N, Vrakking M J J, and Stolow A 2012 *Science* **335** 1336
[27] Mairesse Y, Higuet J, Dudovich N, Shafir D, Fabre B, Mvel E, Constant E, Patchkovskii S, Walters Z, Ivanov M Y *et al.* 2010 *Phys. Rev. Lett.* **104** 213601
[28] Bruner B D, Mašín Z, Negro M, Morales F, Brambila D, Devetta M, Facciala D, Harvey A G, Ivanov M, Mairesse Y *et al.* 2016 *Faraday Discuss.* **194** 369
[29] Diveki Z, Guichard R, Caillat J, Camper A, Haessler S, Auguste T, Ruchon T, Carré B, Maquet A, Taïeb R *et al.* 2013 *Chem. Phys.* **414** 121
[30] Telnov D A, Sosnova K E, Rozenbaum E, and Chu S I 2013 *Phys. Rev. A* **87** 053406
[31] Krause J L, Schafer K J, and Kulander K C 1992 *Phys. Rev. A* **45** 4998
[32] L'Huillier A, Schafer K J, and Kulander K C 1991 *J. Phys. B* **24** 3315
[33] Christov I P, Murnane M M, and Kapteyn H C 1997 *Phys. Rev. Lett.* **78** 1251
[34] Kim H T, Kim I J, Tosa V, Kim C M, Park J J, Lee Y S, Bartnik A, Fiedorowicz H, and Nam C H 2004 *IEEE J. Sel. Top. Quantum Electron.* **10** 1329
[35] Gibson E A, Paul A, Wagner N, Tobey R, Gaudiosi D, Backus S, Christov I P, Aquila A, Gullikson E M, Attwood D T *et al.* 2003 *Science* **302** 95
[36] McFarland B K, Farrell J P, Bucksbaum P H, and Guhr M 2008 *Science* **322** 1232
[37] Smirnova O, Patchkovskii S, Mairesse Y, Dudovich N, and Ivanov M Y 2009 *Proc. Natl. Acad. Sci. USA* **106** 16556
[38] Ren Z X, Zhang B, Yang Y, Zhu Y L, Zhao J, and Zhao Z X 2023 *Results Phys.* **55** 107181
[39] Qiao Y, Zhang S S, Jiang W L, Guo F M, Wang J, Chen J G, and Yang Y J 2025 *Phys. Rev. A* **111** 013501